An Investigation of the Kinematics of Stretch Blow Molding Poly(ethylene Terephthalate) Bottles

MUKERREM CAKMAK,* JAMES L. WHITE,* and JOSEPH E. SPRUIELL, *Polymer Engineering, University of Tennessee, Knoxville, Tennessee*

Synopsis

An experimental study of the kinematics of inflation of poly(ethylene terephthalate) (PET) parisons in a Corpoplast stretch blow molding process is reported. LVDT displacement transducers have been placed at various positions along the length and at the top of a specially designed and built mold. A six-channel LVDT demodular circuit was built and attached to a minicomputer. Studies were conducted at 90 and 100°C at various pressures. Kinematic models were developed for the parison inflation, and stress fields along the deforming surface of the parison were computed using membrane theory.

INTRODUCTION

No process technology has become more important in recent years than that of stretch blow molding polyethylene terephthalate bottles. Since the original patents of Wyeth and Roseveare,[1,2] there have been few published basic studies of the stretch blow molding process.[3-9] In this technology, an extruded or injection molded preform is inflated in both lateral and longitudinal directions at temperatures 25–45°C above the glass transition temperature to fill out the shape of a bottle mold. The multidirectional stretch at these temperatures produces a biaxially oriented bottle. The above-cited previous studies have only roughly investigated the transient kinematics of development of bottle shape, e.g., by inspecting bottle short-shots.[9] Most researchers have been concerned with heat transfer and the mechanisms of pearlescence in bottles.[3-5,7,8]

In the present paper we describe an experimental study of the kinematics of bottle formation using displacement transducers which have been inserted in the mold.

EXPERIMENTAL

Materials

Extruded tubes of polyethylene terephthalate were supplied by American Enka. These had intrinsic viscosities of 0.92 dL/g in 60/40 (wt %) phenol/tetrachloroethane solvent mixture. This corresponds to viscosity averaged molecular weight of 35,000 g/mol. (Mark–Houvink constant: $K = 2.1 \times 10^{-3}$ dL/g and $a = 0.58$.[9] The tubes had outside diameters of 2.5 cm and wall thicknesses of 0.25 cm. Generally lengths of 18 cm were used.

* Present address: Polymer Engineering Center, University of Akron, Akron, OH 44325.

Journal of Applied Polymer Science, Vol. 30, 3679–3695 (1985)
 CCC 0021-8995/85/093679-17$04.00

Bottle Blowing Process—General

The bottle blowing experiments were performed on a Heidenreich and Harbeck Corpoplast laboratory apparatus equipped with a 1-L mold and quartz heaters. A schematic of the process is outlined in Figure 1 (1–6). In step 1, one end of the tube was heated locally by quartz heaters until roughly 1 cm at the end of the pipe is sufficiently softened. Using a hemispherically shaped male and female mold couple, the softened end of the tube was closed (steps 2 and 3). The parison, so-formed, is placed on a mandrel. The open-ended lower portion of the parison was softened with the help of local heating provided by quartz heaters. The softened portion of the parison was pushed over the lowest section of the parison holding stage which has a slightly larger diameter than the inside of the parison.

Upon pushing a start button, an oven begins to pass over the mandrel (step 4). Heating is provided by long horizontal quartz heaters mounted on one wall of the oven. The mandrel rotates as it passes through the oven; this rotation allows for uniform circumferential heating of parison. The temperature profile along the parison was determined using an Ircon infrared pyrometer. This instrument measures a weighted temperature through the parison's thickness. The power to the quartz heaters was manipulated to give a constant temperature along the length of the parison. The mandrel now enters the blowing station. The mold closes around the parison (step 5). High pressure air is now injected, which causes the parison to be stretched simultaneously radially and axially (step 6). The axial displacement is provided by a mandrel driven by the air pressure entering the parison.

Special Mold and Monitoring of Blowing Operation

A special mold was designed and constructed from aluminum for use in this project. Several spring-loaded LVDTs (linear variable differential transformers) were placed along the length of the mold as shown in Figure 2. Five LVDTs were situated to measure the variation of the radius of the parison and one was vertically mounted to determine the length of the

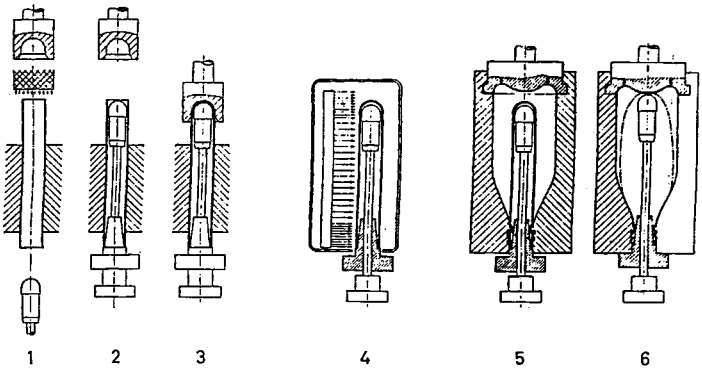

Fig. 1. Steps in Corpoplast stretch blow molding process.

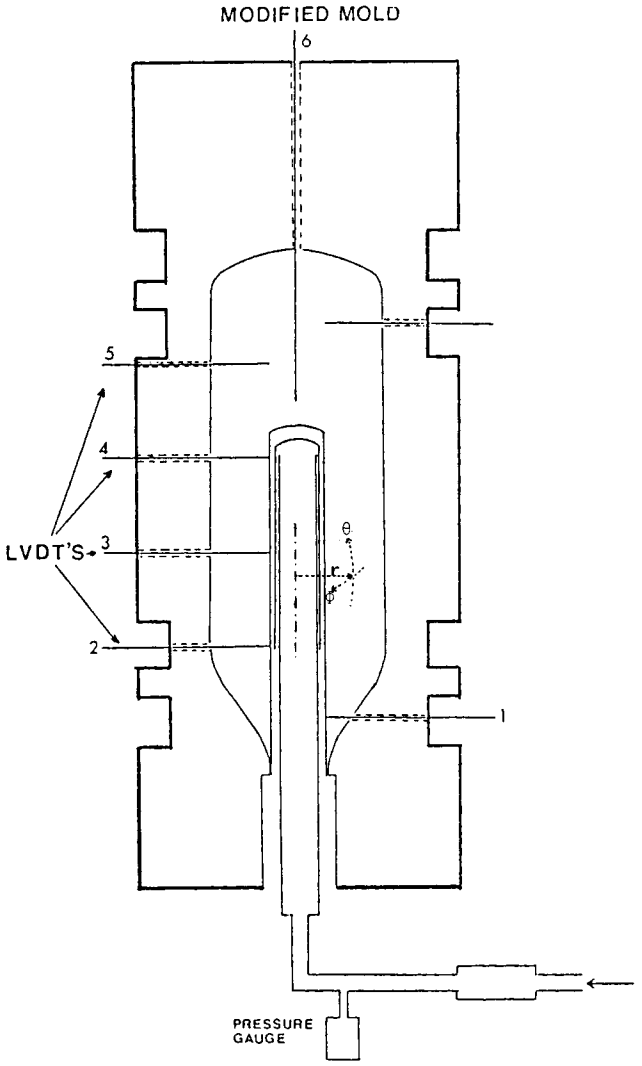

Fig. 2. Specially instrumented mold.

parison. In addition, a Baldwin pressure transducer was placed in the pressure line to follow the pressure history within the parison.

A six-channel LVDT demodulator circuit and pressure transducer panel were designed and built. The LVDT demodulator circuitry and pressure transducer panel were connected to an Applied Micro Technology (AMT) computer through a junction box. The minicomputer was used rather than recorders, because the latter were too slow to respond to many of the variations observed. The minicomputer was capable of reading through A/D converters from eight channels every 4 ms. Data were stored on 8-in. floppy magnetic discs. The final processing and plotting of data were carried out with a Digital Equipment PDP-10 computer.

TABLE I
Conditions of PET Parison Inflation Experiments

Temper (°C)	Pressure [kPa (psi)]
90	413 (60)
90	551 (80)
90	689 (100)
100	275 (40)
100	413 (60)
100	689 (100)

Experimental Conditions

Studies of PET parison inflation were carried out at 90 and 100°C at several different pressures. The specific pressures and temperatures used in the parison inflation monitoring experiments are summarized in Table I.

RESULTS

The inflation pressure of the PET parisons is shown as a function of time in Figure 3 for bottles produced at 90°C. The total final pressure is achieved within 0.8 s. The displacements and displacement velocities of the LVDTs for parisons inflated at 90°C and pressures of 413 and 689 kPa are shown in Figures 4 and 5. The LVDT in position 1 represent the neck of the bottle and those in positions 2–5 various positions along the length leading away from the neck. The LVDT in position 6 represents the axial position of the top of the parison. Considering first LVDTs, 1–5, which measure radial position, we see that the displacements occur successively with positions 1,

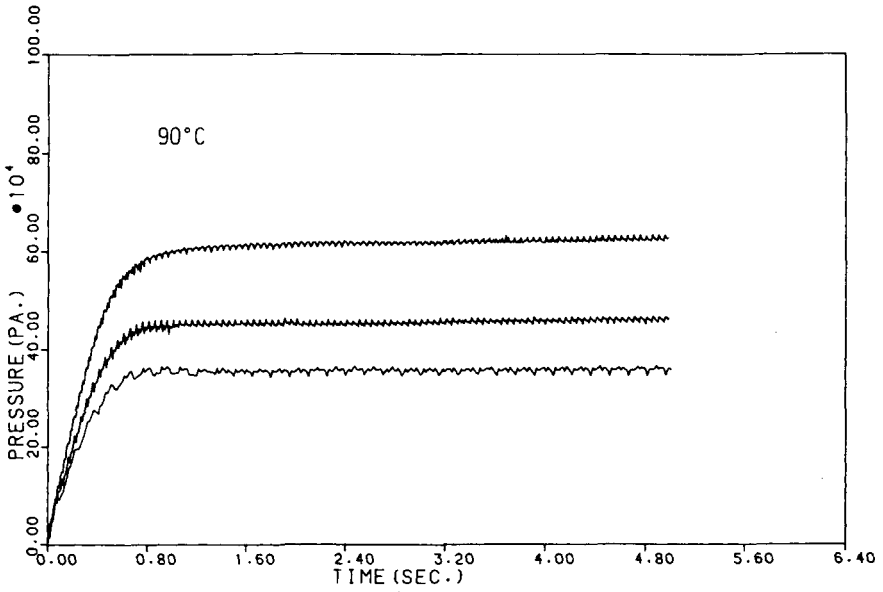

Fig. 3. Inflation pressure as a function of time for parisons inflated at 90°C.

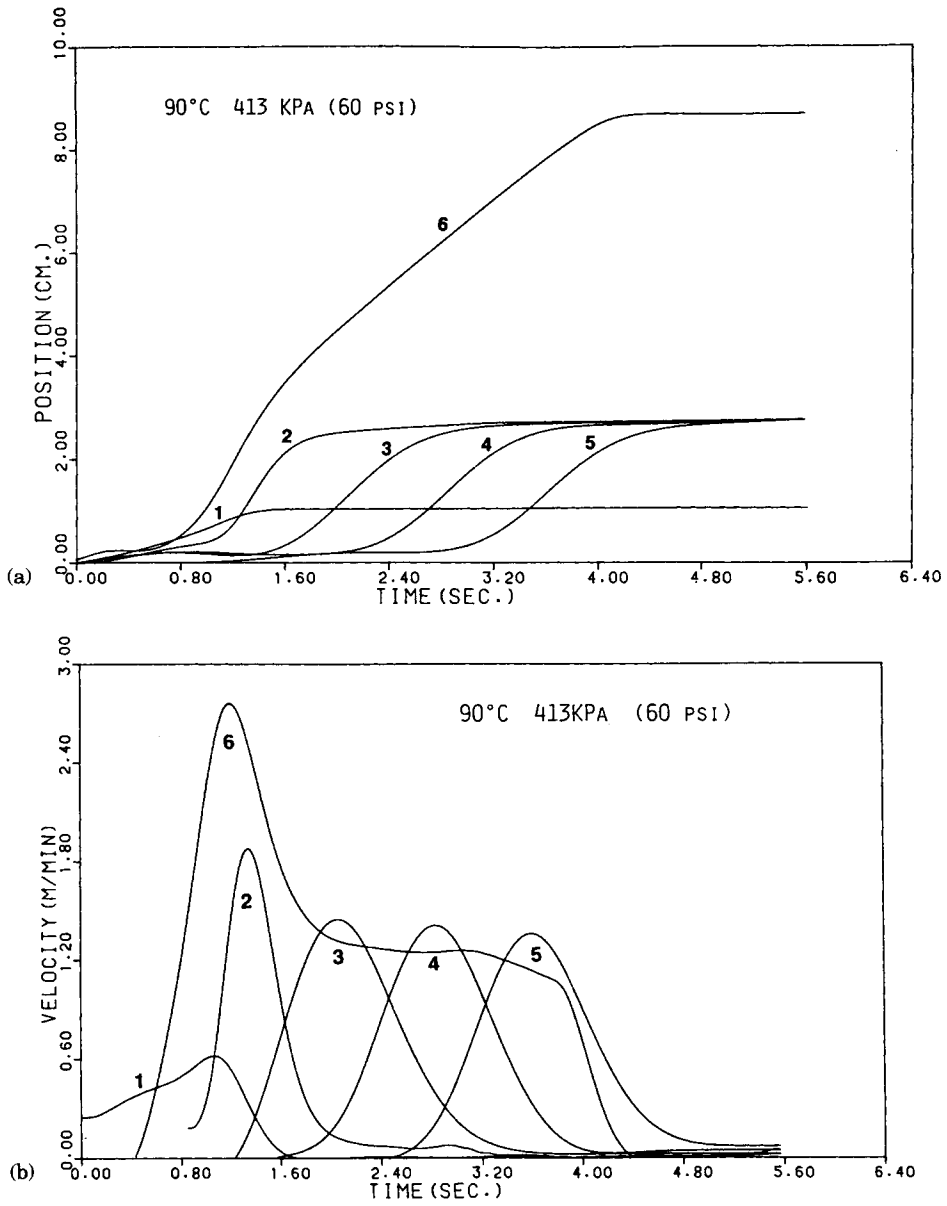

Fig. 4. Monitoring of parison inflation at 90°C and 413 kPa (60 psi): (a) displacement position as a function of time; (b) displacement velocity as a function of time.

2, 3, 4, and 5, i.e., first at the neck and then gradually upward along the bottle axis. Position 1 achieves its asymptotic value at 413 kPa in roughly 1.3 s, position 2 in 2 s, position 3 in 3.2 s, position 4 in 4 s, and position 5 in 4.8 s. The displacement rates at 551 and 689 kPa are accordingly higher and the times required to achieve the desired final positions shorter. The displacement of transducer 6 characterizing the axial height of the center

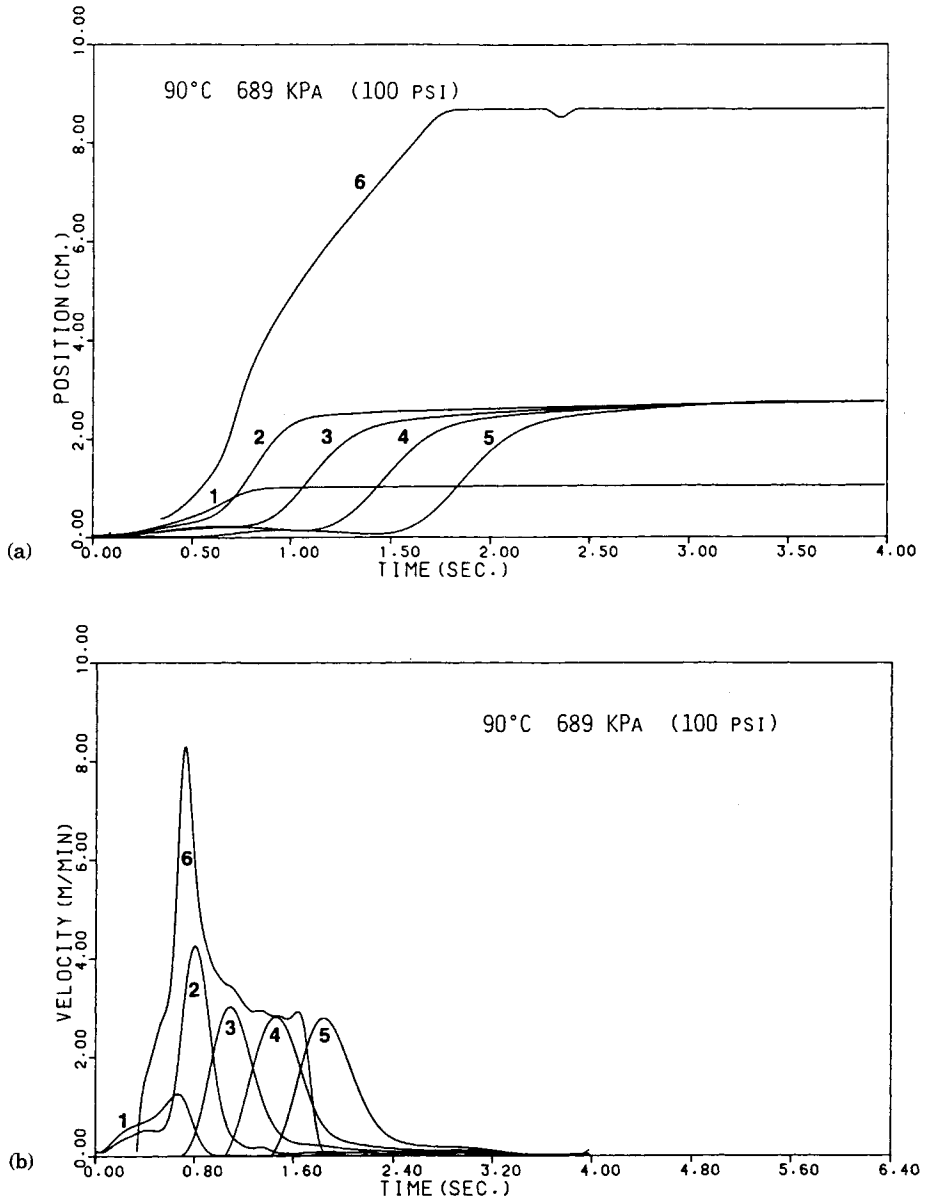

Fig. 5. Monitoring of parison inflation at 90°C and 689 kPa (100 psi): (a) displacement position as a function of time; (b) displacement velocity as a function of time.

of the parison occurs earlier than those along the axis and more rapidly. The behavior at the three different pressure levels studied is the same. The only difference is that, as the pressure is increased, the local velocities and rate of mold filling is increased.

The transient kinematic data for parisons inflated at 100°C are shown in Figures 6–8. Unlike the situation at 90°C where the kinematics are all similar, the behavior at 100°C shows a wide range of differences. The behavior at 275 kPa (40 psi) (Fig. 6) is the same as that at 90°C. However, the

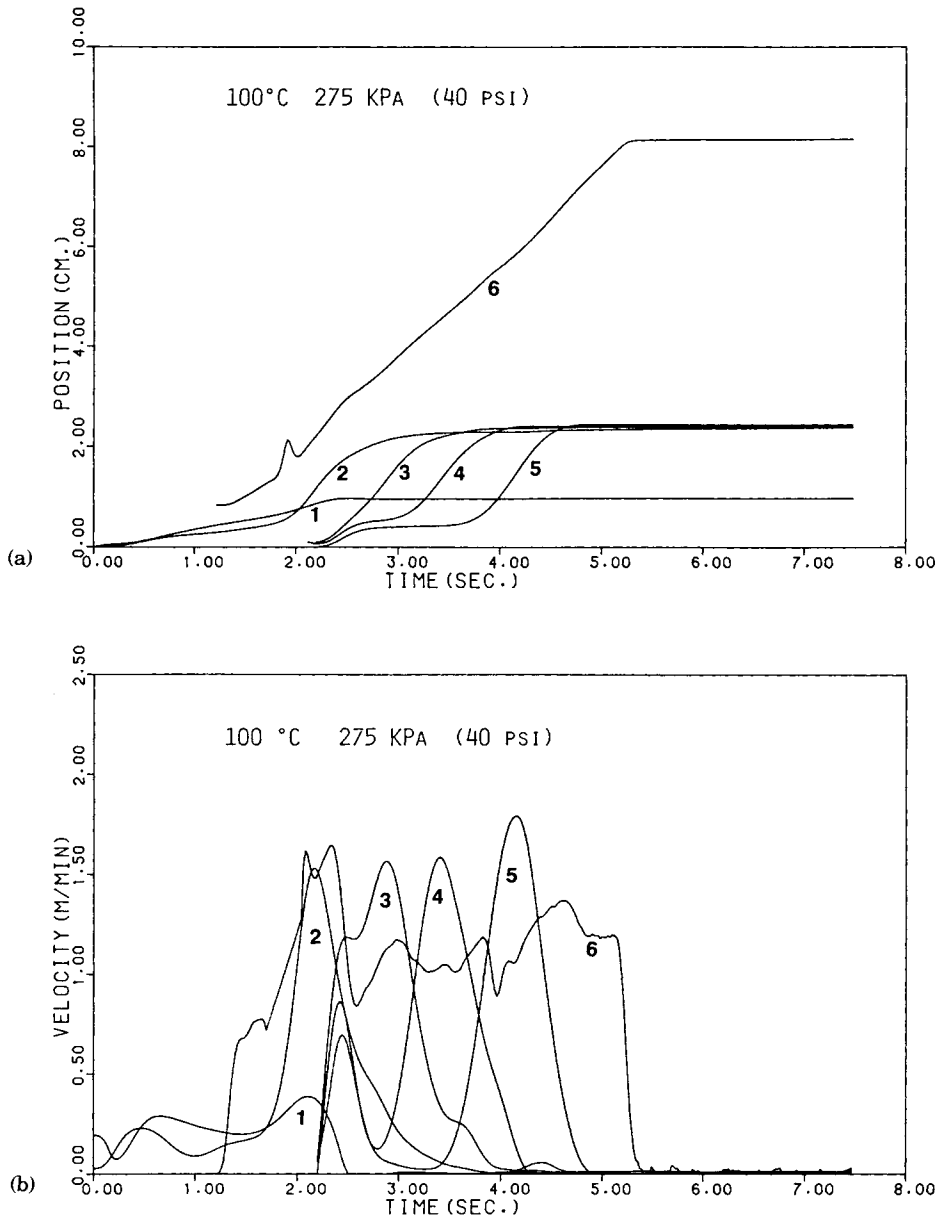

Fig. 6. Monitoring of parison inflation at 100°C and 275 kPa (40 psi): (a) displacement position as a function of time; (b) displacement velocity as a function of time.

responses at 413 kPa (60 psi) shown in Figure 7 is different. Of the LVDTs monitoring radial position, LVDT 4 moves to the maximum position first, 3 is displaced only slightly less rapidly followed by 5 and 2. This displacement of LVDT 1 is generally after that of 2. A third and intermediate type of behavior is found at 689 kPa (100 psi). The first motion is exhibited by LVDTs 1, 2, 3, and 4 simultaneously. This is then followed by successive growth to 90% or more of the total mold radius by LVDTs 2, 1, 3, 4, and 5 successively.

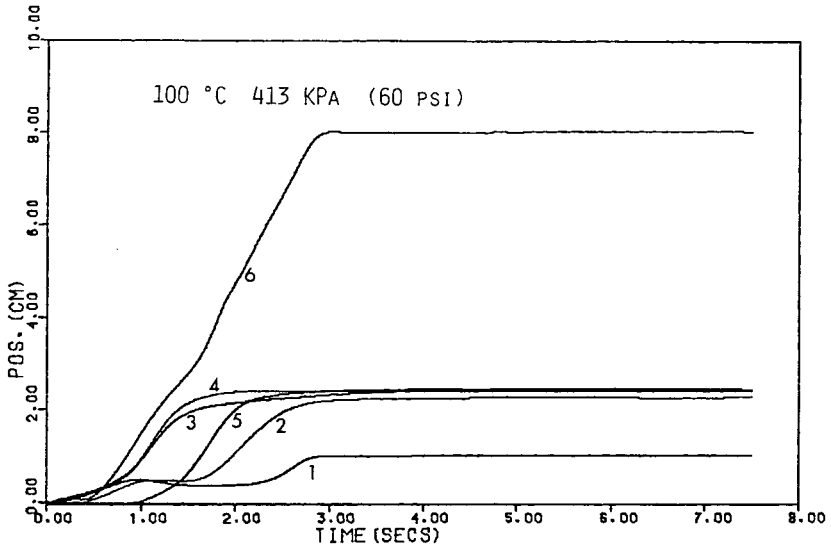

Fig. 7. Monitoring of parison inflation at 100°C and 413 kPa (60 psi). Displacement position as a function of time.

INTERPRETATION

Models of Parison Inflation

It is possible to use the LVDT displacement data of Figures 4–8 to develop models of the mechanism of inflation of the PET parisons. As indicated in the previous section, three distinctly different sets of displacement/velocity time curves are obtained. One set corresponds to all experiments carried out at 90°C as well as at 100°C and 275 kPa (40 psi). Different behavior is

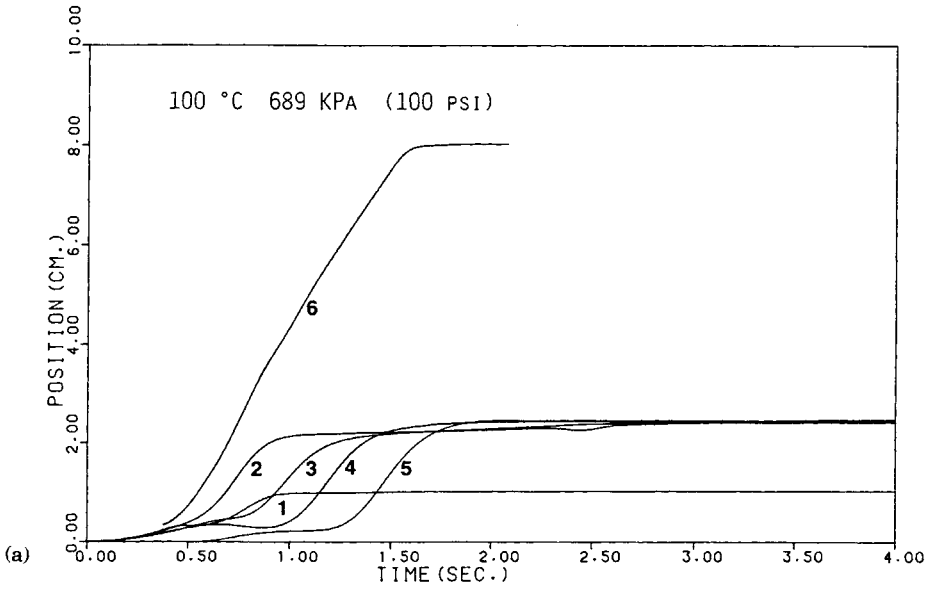

Fig. 8. Monitoring of parison inflation at 100°C and 689 kPa (100 psi): (a) displacement position as a function of time; (b) displacement velocity as a function of time.

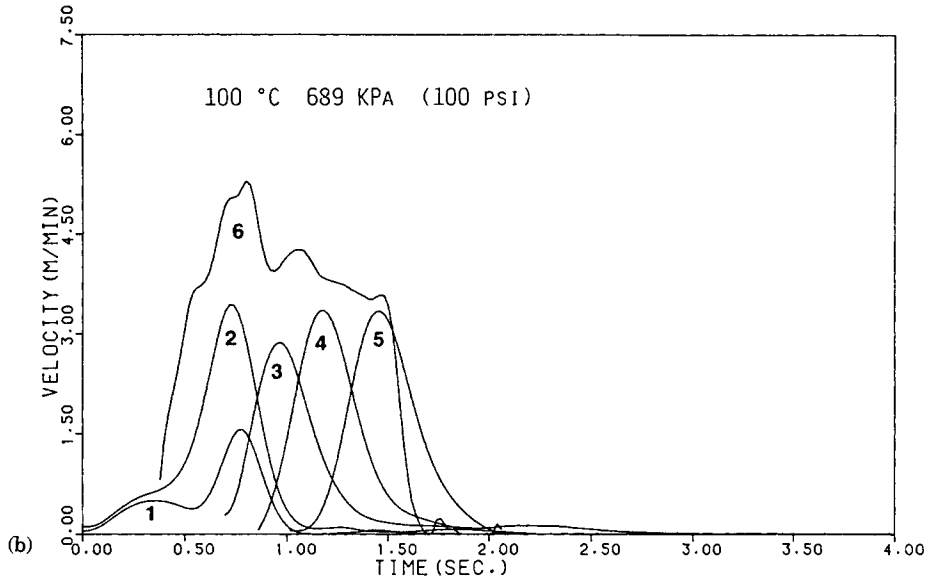

(b)

Fig. 8. *(continued from previous page)*

observed at higher pressures at 100°C inflation temperature. We will first discuss the behavior at the former conditions. The successive position displacements and velocity–time behavior can only be interpreted in terms of the model shown in Figure 9. The parison first inflates to a bubble near the mouth of the bottle. Positions successively higher along the bottle axis then inflate to the full mold radius. This gives the appearance of a front propagating along the bottle axis. As this process continues, the vertical

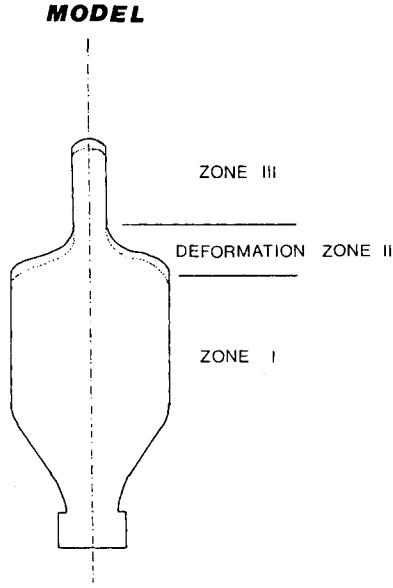

Fig. 9. Model of parison inflation at 90 and at 100°C and 275 kPa.

height of the parison continues to increase at a roughly constant relatively low velocity.

The perspective developed in the above paragraph has been tested by making "short shot" bottles at 90°C and 551 kPa. The results shown in Figure 10 support our displacement transducer experiments and interpretation.

The observations at higher pressures at 100°C require separate interpretation. The results of Figure 7 corresponding to 100°C and 413 kPa (60 psi) indicate the displacement transducers moving to a maximum position in the order of LVDTs 4, 3, 2, 1. This must indicate that a bubble is first formed at an intermediate axial position and then simultaneously propagates vertically upwards and downwards. This view is summarized in Figure 11.

The behavior at 100°C and 689 kPa requires a third model of parison inflation. Here all of the LVDTs translate at about the same velocity for a short period followed by rapid succession of LVDTs 2, 1, 3, 4 and 5. This suggests the behavior shown in Figure 12. The parison first shows a general uniform inflation. A bubble then grows near the mouth and propagates vertically upward (and downward) filling the mold.

Stress Field of the Inflating Parison—General

It is possible to compute the stress distribution in the inflating parison using the methods of membrane theory. For an arbitrary axisymmetric membrane the balance of forces may be expressed as[11]

$$\frac{d}{d\theta}(rN_\theta) - r_1 N_\phi \cos\theta + p_\theta r r_1 = 0 \tag{1a}$$

$$\frac{N_\theta}{r_1} + \frac{N_\phi}{r_2} = p_r \tag{1b}$$

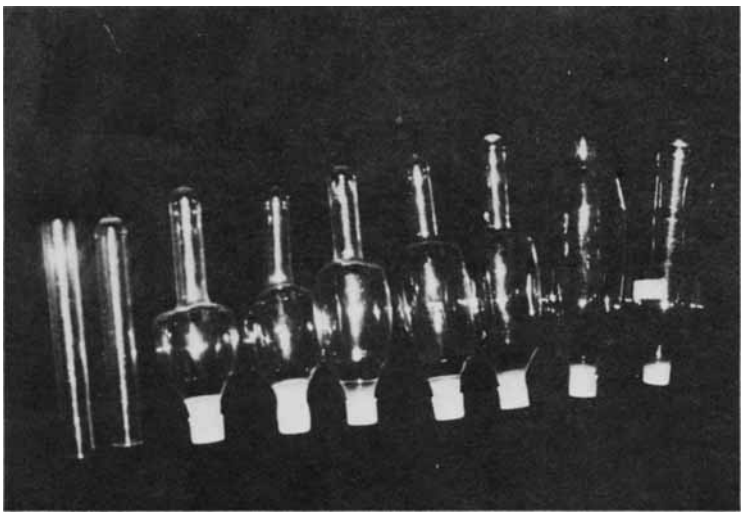

Fig. 10. PET short shot bottles produced at 90°C and 413 kPa.

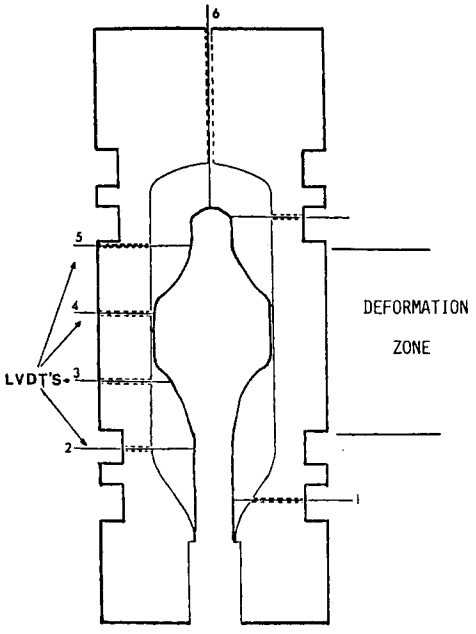

Fig. 11. Model of parison inflation at 100°C and 413 kPa.

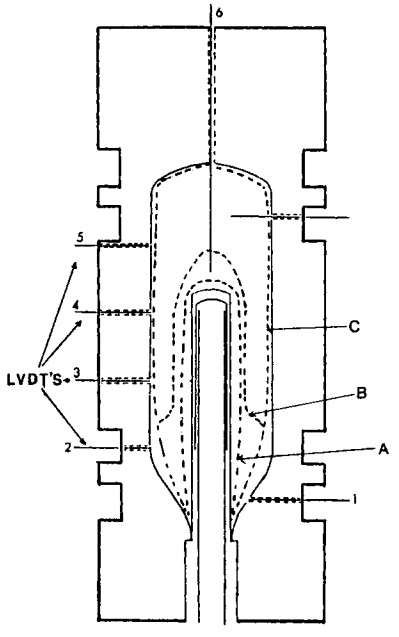

Fig. 12. Model of parison inflation at 100°C and 689 kPa.

Here N_θ is the force per unit length in the θ (meridional direction), N_ϕ the force per unit length in the circumferential direction, and r_1 and r_2 the corresponding radii of curvature. P_r is the inflation pressure and p_θ a body force in the θ (meridional) direction. If gravity is neglected, p_θ is zero. r is the local radius.

We may solve eqs. (1a) and (1b) simultaneously to yield the quantities N_θ and N_ϕ as a function of position along the length of the bottle if the inflation pressure and shape are known. Neglecting gravity, we obtain

$$N_\theta = \frac{1}{r_1 \sin^2 \theta}\left[\int r_1 r_2 p_r \cos \theta \sin \theta \; d\theta + C\right] \tag{2}$$

and N_ϕ is obtained from eq. (1b). Integration of eq. (2) leads to

$$N_\theta = \frac{1}{2r \sin \theta}\left(pr^2 + \frac{F}{\pi}\right) \tag{3a}$$

$$N_\phi = \frac{r}{\sin \theta}\left[p - \frac{N_\theta}{(1/\cos \theta)\, dr/d\theta}\right] \tag{3b}$$

where we write p_r as p.

Along the cylindrical section of the finished bottle, θ is 90 and

$$N_\theta = \frac{pr}{2} + \frac{F}{2\pi r} \tag{4a}$$

$$N_\phi = pr \tag{4b}$$

In the absence of axial force F, these equations [(4a),(4b)] further reduce to the classical pressure vessel solution.

Determination of N_θ and N_ϕ

The kinematic data for bottles blown at 90°C suggests the deformation model presented in Figure 9. In zone I the parison has already deformed, and no further deformation occurs. The deformation is localized in zone II which depicts the deformation front.

Since no deformation is assumed to take place in zone III, the axial displacement data (LVDT 6) can be taken as axial displacement of the deformation front. For a given small time interval (Δt), this provides Δz. Since the system is in a steady state condition in the cylindrical section of the mold, the radially mounted LVDT 3 essentially traces the shape of this propagating deformation front and provides radius as a function of time. The meridional angle can thus be determined from

$$\theta = \tan^{-1} \frac{\Delta z}{\Delta r} \tag{5}$$

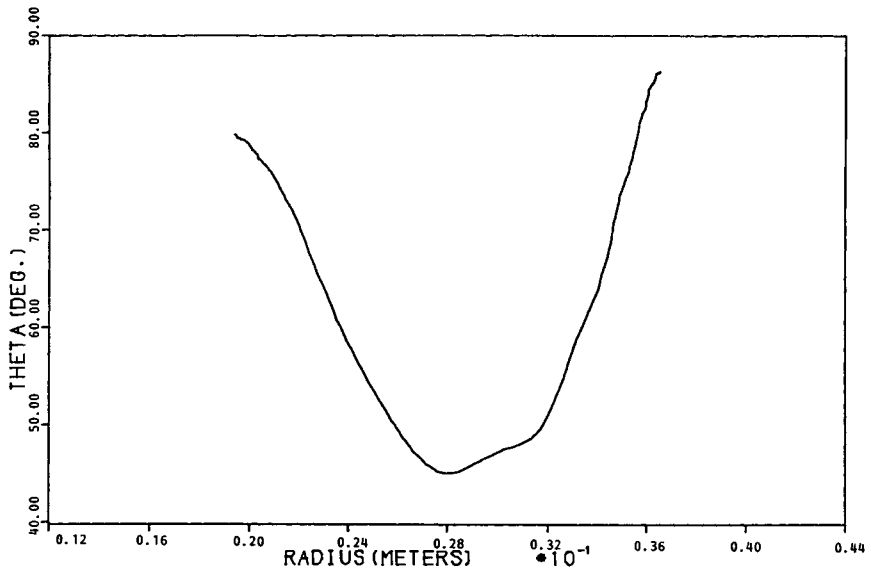

Fig. 13. Experimentally determined θ as a function of radius on the deformation one.

Figure 13 depicts a typical experimentally determined as a function of radius in the deformation zone. This angle θ decreases to about 45° and then increases with the increase of radius reaching 90° at the final radius of 4 cm. The axial force F in eq. (3a) may be determined from the internal pressure and contact area of the mandrel with parison end.

We have computed N_θ and N_ϕ for bottles blown at 90°C at 413 kPa (60 psi). We present this in Figures 14 and 15 for both LVDT 3 and 4 position. These figures show little differences between data from positions 3 and 4.

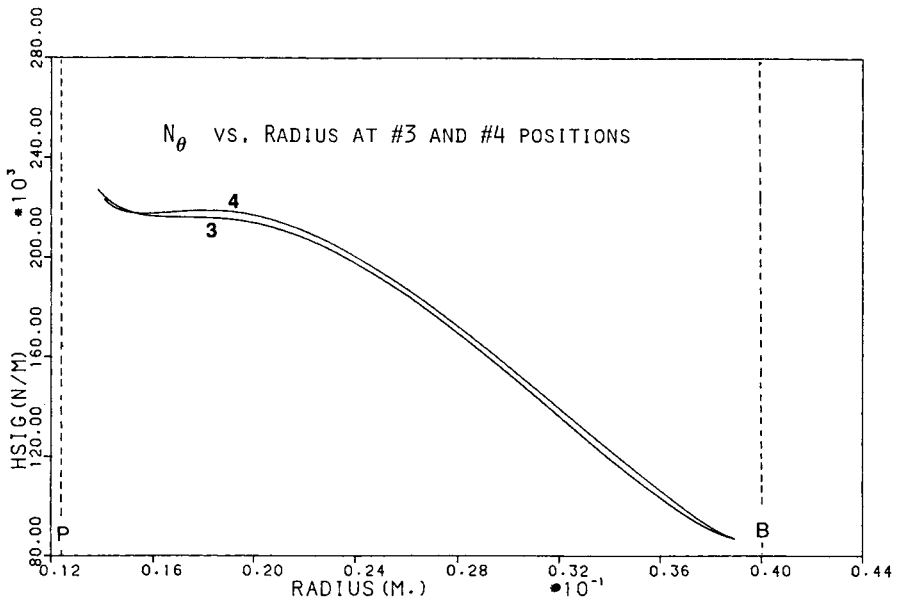

Fig. 14. Computed N_θ as a function of radius in deformation zone. P = Parisan radius, B = Bottle radius.

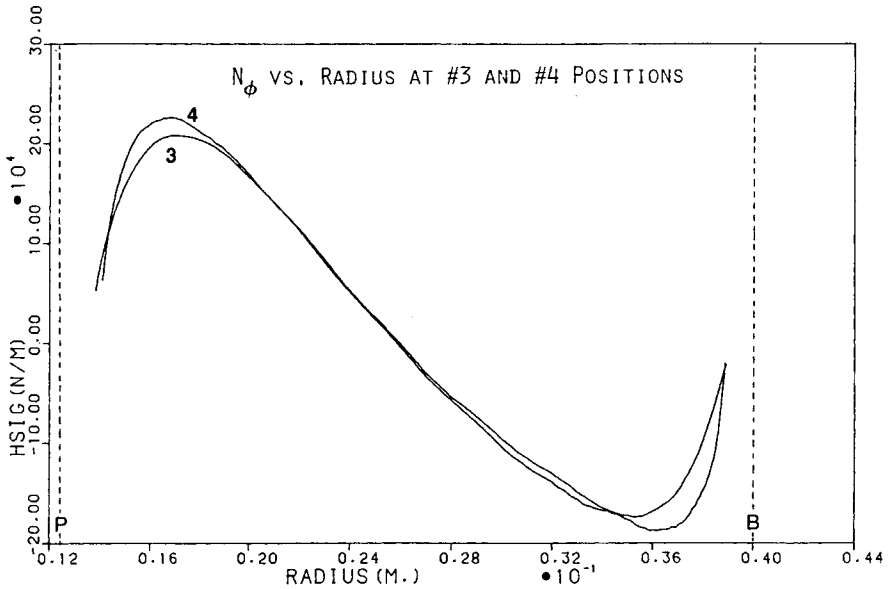

Fig. 15. Computed N_ϕ as a function of radius on the deformation zone. P = Parison radius, B = Bottle radius.

This is an additional proof that the deformation front propagates in a steady state fashion in the cylindrical regions of the mold.

N_θ (meridional force per unit length) decreases with increasing radius after an initial plateau region. On the other hand, N_ϕ (circumferential force per unit length) first increases with radius exhibiting a maximum and then becomes negative approaching zero at the mold wall. This is attributed to a sign change in $dr/d\theta$ (Fig. 13) at large radius. At small r, $dr/d\theta$ is negative, making the second term in parenthesis in eq. (3b) positive. On the other hand, at large radii, $dr/d\theta$ is positive, and this results in negative N_ϕ values. In Figure 16, we illustrate this schematically by plotting N_θ and N_ϕ as a function of position along the bottle axis beside a schematic of the bottle deformation zone. Wrinkling is observed in the circumferential direction in the deformation zones of short shot bottles.

Figures 17 and 18 depict the effect of operation pressure on N_θ and N_ϕ for 3 position in the mold. In general, higher stresses are achieved in N_θ and N_ϕ of a given radius with increase of blowing pressure.

We also plotted the difference $N_\theta - N_\phi$ as a function of position (radius) for position 3 for bottle blown at 90°C with 413 kPa (60 psi) (Figure 19). This plot indicates that most of the length of the parison is dominated by the meridional stresses.

Kinematics and Probable Temperature Rise

As found in our kinematic data, the material encounters high stretch rates during the blowing operation. The maximum rates range between 250 s^{-1} (15,000%/min) and 416 s^{-1} (25,000%/min), depending on the level of processing temperature and pressures. With these high deformation rates, the time to complete blowing ranged from 3 to 6 s. This high mechanical energy imposition on the material is expected to cause an adiabatic heating.

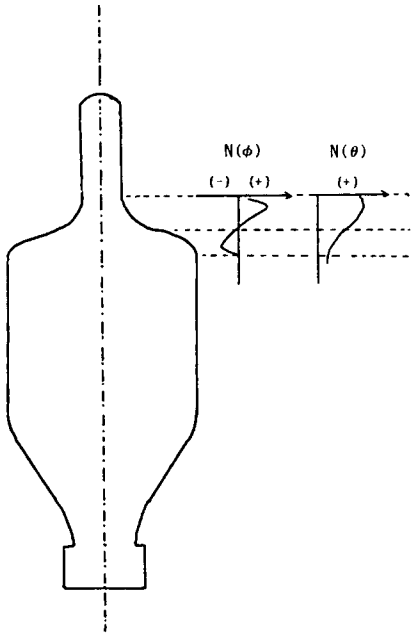

Fig. 16. Schematic of bottle and N_θ and N_ϕ as a function of axial position.

Because of the geometrical restrictions of our mold, we could not determine this behavior experimentally. However, we can estimate it. Stresses of order 5×10^7 Pa develop with stretch rates of order 300 s^{-1}. In the adiabatic approximation

$$\rho c \frac{\partial T}{\partial t} = \sigma_{\theta\theta} d_{\theta\theta} + \sigma_{\phi\phi} d_{\phi\phi} + r(\Delta H) \tag{6}$$

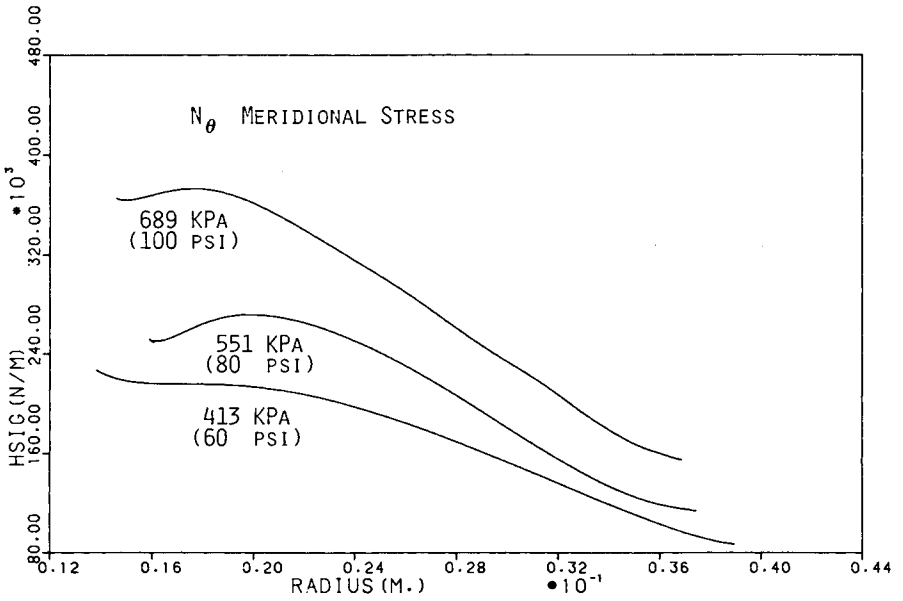

Fig. 17. Effect of pressure on N_θ vs. r.

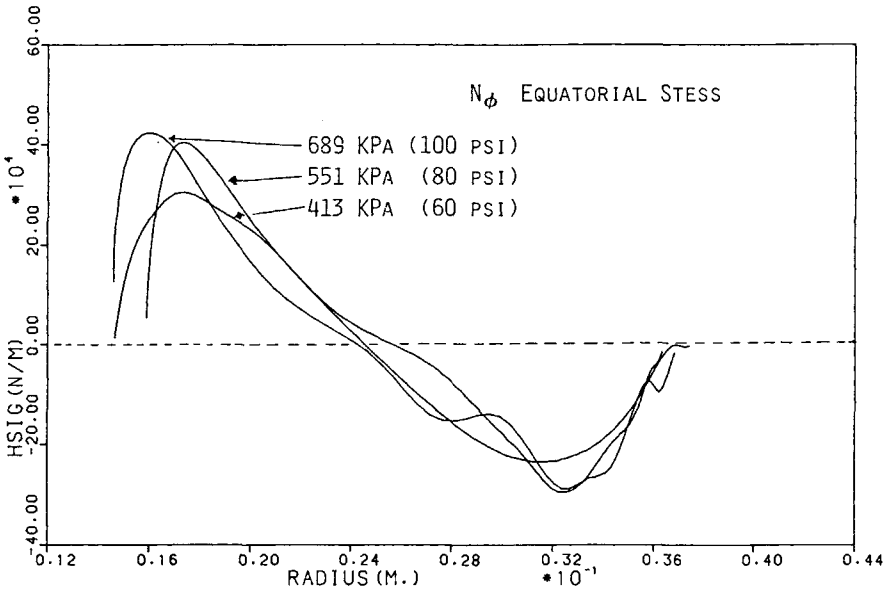

Fig. 18. Effect of pressure on N_ϕ vs. r.

where ρ is density, c is heat capacity, $\partial T/\partial t$ is the rate of temperature rise, σ_{ii} and d_{ii} are stress and deformation rate components, and $r(\Delta H)$ is the heat evolution through crystallization. This suggests adiabatic rates temperature increase of order 16,000°C/s without considering crystallization ($C=0.33$ cal/g°C, $\rho=1.335$ g/cm^3). The actual heating rate would be much less. Bonnebat et al.[6] stretched a PET film kept at 95°C oven uniaxially at (0.5 s^{-1}) 30%/min. They observed a 15°C increase in temperature of a sample within 3 s of deformation. Recently, Warner[12] also found similar results in uniaxial stretching of PET and added that this temperature rise is due to two factors. One is plastic deformation associated with neck formation and propagation, and the second factor is due to crystallization.

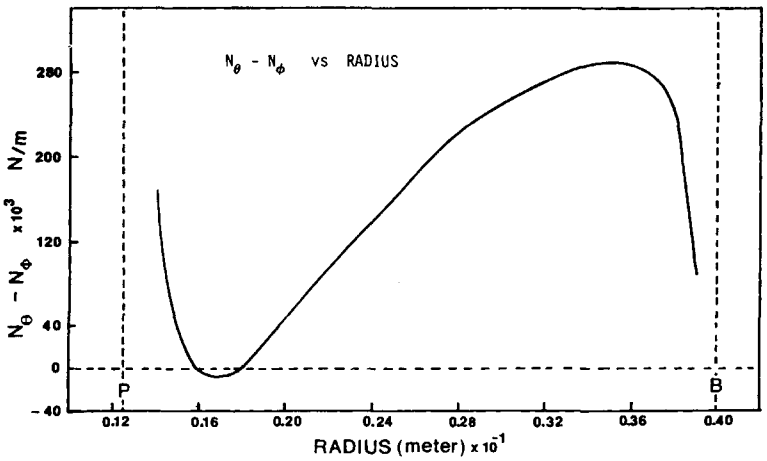

Fig. 19. $N_\theta - N_\phi$ as a function of radius at the deformation zone for position 4. P = Parison radius, B = Bottle radius.

The above general behavior indicates that thermal history of the stretch blow molded PET bottles are quite complex. In the initial state, the parison encounters a heating and cooling (equilibration) cycle and during the blowing the material encounters adiabatic heating due to deformation and stress induced crystallization and finally cooling due to contact at the mold wall.

References

1. N. Wyeth and R. N. Roseveare, U.S. Pat. 3,733,309 (1973).
2. N. Wyeth and R. N. Roseveare, U.S. Pat. 3,849,536 (1974).
3. H. G. Fritz, *Kunststoffe*, **68**, 450 (1978).
4. B. Miller, *SPE Antec Tech. Pap.*, **26**, 540 (1980).
5. H. G. Fritz, *Kunststoffe*, **71**, 687 (1981).
6. C. Bonnebat, G. Roullet, and A. J. de Vries, *Polym. Eng. Sci.*, **21**, 189 (1981).
7. S. L. Kim, *Polym. Eng. Rev.*, **4**, 239 (1984).
8. S. L. Kim, *Polym. Eng. Rev.*, to appear.
9. L. Erwin, M. A. Pollock, and H. Gonzalez, *Polym. Eng. Sci.*, **23**, 826 (1983).
10. J. Brandrup and E. H. Immergut, *Polymer Handbook*, Wiley-Interscience, New York, 1966.
11. W. Flugge, *Stresses in Shells*, Springer-Verlag, Berlin, 1960.
12. S. B. Warner, *J. Appl. Polym. Sci.*, **29**, 219 (1984).

Received October 25, 1984
Accepted January 17, 1985